A systematic methodology for optimal integration of heat pumps in industrial processes

Rafael Simonetti Bullio[a], Gilles Hetreux[b], Raphaële Thery Hetreux[c]

[a]Laboratoire de Génie Chimique, UMR 5503, Toulouse, France, rafael.simonettibullio@toulouse-inp.fr
[b]Laboratoire de Génie Chimique, UMR 5503, Toulouse, France, gilles.hetreux@toulouse-inp.fr
[c]Laboratoire de Génie Chimique, UMR 5503, Toulouse, France, raphaele.thery@toulouse-inp.fr, CA

Abstract

The approach consists of three main stages: First, a Pinch Analysis determines the coordinates of the Grand Composite Curve (GCC), which serve as inputs to the optimization model. A Mixed-Integer Linear Programming (MILP) model is then used to determine the heat pumps' operating temperatures that maximizes system exergy efficiency. Second, based on the calculated temperatures level, the "Robust software tool for the synthesis of Flexible Heat Exchanger Networks" (RREFlex) — also relying on a MILP formulation — determines the optimal topologic placement of the heat pumps i.e., the corresponding process hot and cold streams connections. Finally, the fluid of the heat pump is chosen to be consistent with the heat pumps' evaporator and condenser operating temperatures used to implement Based on all these parameters, a ProSimPlus simulation model is developed to refine the operating temperature while accounting for the influence of temperature on the thermal properties of the process streams.

Keywords

Heat Pumps; Pinch Analysis; Heat Exchanger Network; Simulation; Biodiesel.

1. Introduction

The industrial sector faces major challenges in achieving carbon neutrality by 2050. According to the International Energy Agency (IEA), the industrial sector directly emitted 9.0 gigatons (Gt) of CO_2 in 2022, accounting for 25% of global energy system CO_2 emissions and 37% of total global energy consumption [1]. During COP30, which took place in Belém, Pará, Brazil, in November 2025, 56 consensus decisions reaffirmed commitments to advancing global climate action [2]. In this context, heat pumps (HPs) represent a promising solution to reduce energy imports and strengthen process energy integration. Their use allows industrial processes to operate below the minimum energy requirement identified through pinch analysis, thereby lowering both hot and cold utility demands by partially replacing them with electricity consumption [3]. As a result, integrating a heat pump into an industrial process can substantially improve energy efficiency and support decarbonization goals. However, determining the appropriate number and placement of heat pumps remains a challenging task that requires a systemic analysis of the overall process. Energy integration, broadly defined as the systematic reuse of energy flows within or between industrial processes, is a fundamental and well-established strategy that enables this systemic analysis by targeting the Minimal Energy cold and hot utility requirement. [4] Moreover, the use of the Grand Composite Curve (GCC) [5] enables to select utilities the that best meet process requirements while minimizing energy losses.

Utilities include furnaces, cogeneration systems that combine heat and power production and heat pumps that use electricity to upgrade existing low-temperature thermal streams to higher temperature enabling their reuse into the process. Many studies illustrate how the Grand Composite Curve (GCC) can be used to determine the number of heat pumps to install as well as their placement within the process, that is, the condensation and evaporation temperatures of each heat pump [6]. However, at this stage, the GCC does not provide the topological integration of the condensers and evaporators within the process i.e., the specific process streams connected to the heat pump. Moreover, it should be recalled that the placement derived from the GCC assumes that the process operates at the Minimum Energy Requirement (MER). Yet, it is well known that the heat exchanger network corresponding to the MER is not necessarily the one that best balances energy savings and investment costs.

This study aims to address this limitation by introducing a generic and systematic methodology starting from the analysis of the GCC and ending with the simulation of the process including heat pump and corresponding to a good compromise between energy recovery, capital cost and complexity. The methodology is then applied to an illustrative case study.

1.1. Energy integration considering heat pumps

Heat pumps are devices that upgrade heat from a low to a high temperature level using an external energy source. Practically, this operation relies on the evaporation and condensation of a refrigerant fluid circulating in a closed loop. Operating on a compression cycle, the heat pump extracts heat in the evaporator (see Figure 1, transition between points 1 and 2), where the refrigerant absorbs heat and vaporizes. This resulting vapor raising both its pressure and temperature. The thermal energy is then released in a condenser liquid (transition between points 3 and 4 in Figure 1) where the refrigerant condenses while transferring heat to another fluid. An expansion valve subsequently lowers the refrigerant's pressure, allowing it to return to the evaporator and restart the cycle. In this way, the system transfers thermal energy using the electrical energy consumed by the compressor [5]. An HP uses a coefficient of performance (COP) to measure this conversion. The COP is the ratio of the thermal energy released at the condenser (Q_{cond}) to the electrical energy consumed by the compressor (W_{elec}) to operate the HP (COP = Q_{cond} / W_{elec}). A high COP indicates high efficiency, meaning that the HP delivers several times more thermal energy than it consumes in electrical energy. The COP significantly depends on the operating conditions, especially the temperatures of the cold and hot sources.

Process HP that are studied in this paper connect refrigerant to process streams in both evaporator and condenser heat exchanger. Figure 1 shows a schematic representation of this configuration. The black lines represent the process streams, and the purple lines represent the refrigerant circulating within the HP cycle. Process HPs interact with the process streams at both heat exchangers. Concerning their temperature placement, HPs are typically positioned between two zones of the GCC around the process pinch point.

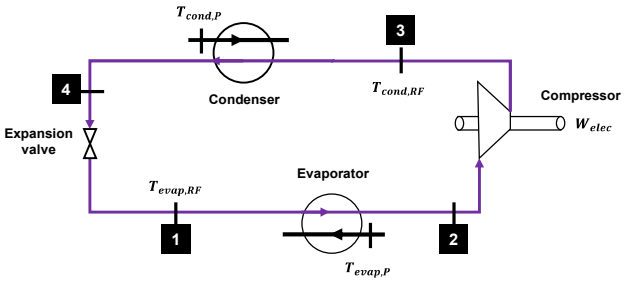

Figure. 1. *Process heat pump diagram.*

2. Proposed methodology

The methodology introduced in this study is structured into three main stages for determining the HP parameters and the optimal number of units, as depicted in Figure 2. Its originality comes from the combination of these steps, which leverage and adapt established models and simulation tools from the literature.

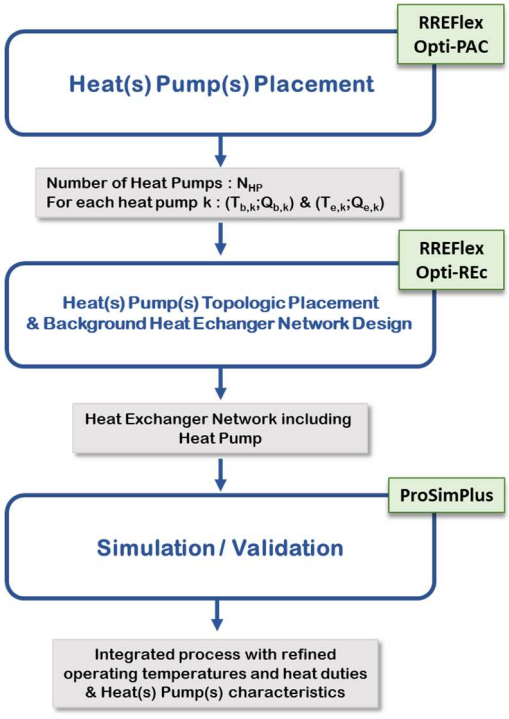

Figure. 2. *Main steps of proposed methodology.*

The first stage involves determining the number of heat pumps and their operating temperatures. To achieve this, the methodology starts with a *Pinch Analysis* to derive the *Grand Composite Curve* (GCC). The ècoordinates of the GCC are then used as inputs for a first *Mixed-Integer Linear Programming* (MILP) model. This model identifies the heat pump operating temperature that maximizes system's exergy efficiency, within the Opti-PAC tool.

The second stage relies on the *RREFlex software* [7], which was developed at the Laboratoire de Génie Chimique and formulated as a MILP formulation determines the optimal placement of the heat pump and the corresponding connections to the process streams is Based on the temperature level identified in the previous stage. This model has been into the RREFlex software as an extension for placement HPs and is named Opti-REc. It is connected to the main module to perform the synthesis of a Heat Exchanger Network (HEN) integrating one or several heat pumps.

In the third and final stage, the fluid of the heat pump is chosen to be consistent with the heat pumps' evaporator and condenser operating temperatures and a ProSimPlus simulation model is deduced from all these parameters to refine the operating temperatures while accounting for the influence of temperature on the thermal properties of the process streams.

This ensures physical consistency of the overall solution.

2.1. Heat pump placement

The thermal placement of the heat pumps is examined in a two-part analysis that adapt a model introduced by [8]. First, the process streams are used to carry out a data pre-processing step from which the *Grand Composite Curve* (GCC) is derived computation. The GCC coordinates are then used as inputs to the MILP model, which calculated the heat pumps' optimal thermal characteristics.

2.1.1. The *Grand Composite Curve* (GCC) as input data

To perform the GCC, the input parameter includes the mass flow (F), specific heat capacity (Cp), inlet temperature (T_{in}), and outlet temperature (T_{out}) values for each flow. In addition, the minimum temperature difference (ΔT_{min}) between the hot and cold flows must be specified. This value can be specified as either a global ΔT_{min} [9] or a local ΔT_{min} [5], where each flow can have its own ΔT_{min} value.

Pinch analysis aims to identify the minimum consumption of external energy and maximize internal heat recovery between the hot and cold streams of an industrial process. This analysis makes it possible to determine the *main pinch point*, which is the point of zero heat required and corresponds to the smallest distance between the hot and cold composite curves. The pinch point divides the system into two thermally independent subnetworks. Above the pinch point, the process requires external heat input (hot utility), while below it, excess heat must be removed (cold utility). Therefore, any heat transfer across this point increases utility consumption and violates the objective of maximum energy recovery.

The results can be represented using the GCC, which provides an overview of the potential for thermal integration by plotting the cumulative energy balances of all heat sources and the heat requirements of the various process streams on a single temperature axis. The GCC graphically highlights the amount of energy that can be recovered or supplied at each temperature level. An example of GCC is illustrated in Figure 3.

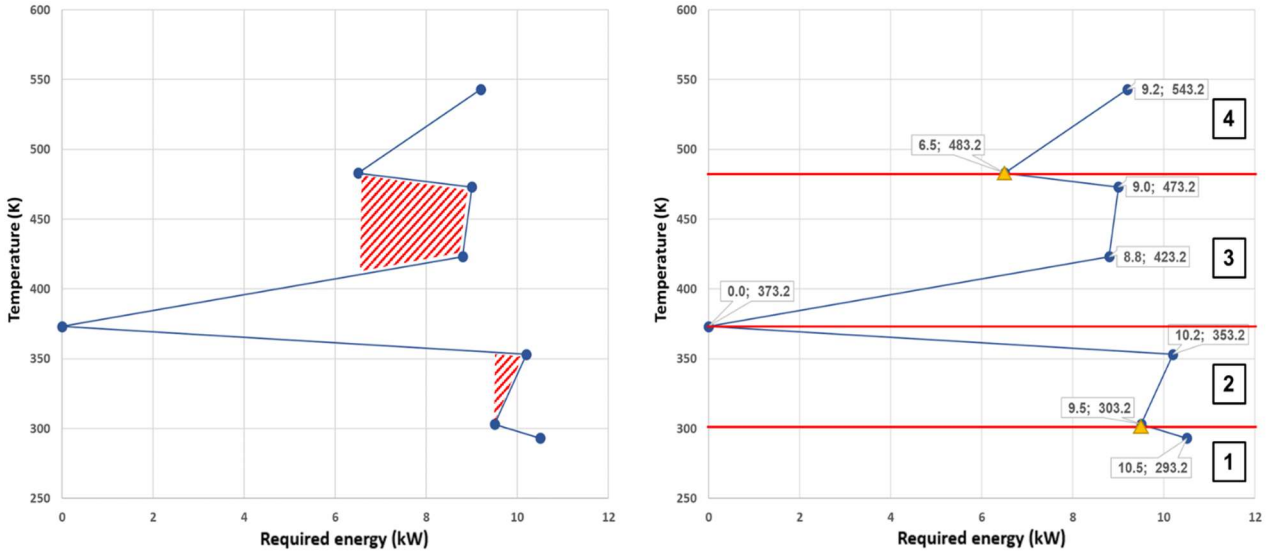

Figure. 3. *Graphical example illustrating the Great Composite Curve (GCC): a) GCC with focus on pockets of heat recovery, b) GCC with identification of 2 utility pinch and the different zones.*

Looking at the curve, the extremes indicate the minimum requirements for hot (at the top) and cold (at the bottom) utilities. These quantities cannot be met through internal recovery and must be supplied or extracted from external sources. Pockets of heat recovery can be identified by the red shaded area in Figure 3a. These areas correspond to regions of the curve where there is a local energy surplus and deficit, meaning they are self-sufficient zones. Performing a HEN between these temperatures using only integration heat exchangers is possible, which do not require external inputs (i.e., cold and hot utilities). Similar points to the pinch point are also indicated by yellow triangles in Figure 3b, but they have non-zero associated energies. These points are called utility pinch [5]. It should be noted that the utility pinch are intrinsically linked to the presence of heat recovery pockets: if the utility pinch lies above the pinch temperature, the corresponding heat recovery pocket lies below it; if the utility pinch lies below the pinch temperature, the heat recovery pocket is above it. For the example, both situations can be observed.

The first step of the model involves using the GCC coordinates obtained from Pinch Analysis. These coordinates are then pre-processed to identify potential pinch points (PPP), which include the main pinch point and utility pinch points. In the example shown in Figure 3b, the main pinch point is located at (0.0, 373.2), while the utility pinch points are identified at (6.5, 483.2) and (9.5, 303.2). This identification uses an algorithmic criterion: a PPP is identified when a sequence of three consecutive points shows a decrease in enthalpy, followed by an increase as the temperature rises. Based on these points, the total number of zones (z) is defined as the number of PPP plus one. The GCC in Figure 3b is then divided into four zones, each of which corresponds to a specific temperature interval separated by red horizontal lines. Each zone is then divided into segments, i.e., temperature points inside a zone. At the end of this stage, the zone and segment associated with the pinch point are identified and stored, since the equations differ above and below this point due to its singular thermodynamic role. This pre-processing step therefore assigns each temperature in the GCC a zone and segment number, in the example presented in Figure 3b, zone 1 has 1 segment, zone 2 has 2 segments, zone 3 has 3 segments, and zone 4 has 2 segments.

These values then undergo a discretization operation: whereby a maximum permissible temperature difference between 1 and 5 K is typically set between two successive points. This enables intermediate points to be inserted and refines the division of the curve. This process is particularly important for positioning HP in contexts where the temperature difference between the evaporator and condenser is low. This approach results in a complete renumbering of the segments to maintain consistent numbering. Ultimately, the total number of all zones (Z), the total number of segments (k ranging from 1 to S_z for each zone Z), and the maximum number of segments in a given zone are all defined.

This entire pre-treatment process has been refined together with the pinch analysis within the Opti-PAC module to make the engineer's job more efficient.

2.1.2. The MILP model for heat pumps

The mathematical model adopted to determine the optimal position and the respective characteristics is based on [8]. However, the model presented in the aforementioned publication contains simplifications that necessitated adjustments in order to account for more complex HP position scenarios. While the original article includes models for additional utility systems, only the equations pertaining to heat pumps were considered in this work.This section describes the equations that have been modified compared to the reference model.

The first change concerns the amount of energy recovered in the evaporator ($Qevap_{y,j}$) positioned in the zone y and the segment j, is directly linked to the available heat at this temperature in the GCC. The amount of heat released in the condenser ($Qcond_{z,k}$) positioned in the zone z and the segment k, can be calculated using the COP definition; for the presented model, this is given by Eq. (1).

$\forall\, z \in [\text{ZonePinch}, Z], \forall\, k \in [1, S_z]$

$$Qcond_{z,k} = \sum_{y \in [1,\, ZonePinch-\,],\ j \in S_y} Qevap_{y,j} * \frac{COP_{y,j,z,k}}{COP_{y,j,z,k} - 1} \qquad (1)$$

Once the HP has been positioned, the new GCC values (NHL) must be recalculated to account for its effect. As previously described, adding a HP reduces energy demand [3]. The design principle of the GCC must be preserved, which means that all enthalpy values must be greater than or equal to zero. Eq. (2) and Eq. (3) present the NHL updates. Eq. (2) relates to the update below the pinch point and takes into account the previous GCC values (Q) minus the amount of heat recovered ($Qevap$) by the HP positioned. Eq. (3), on the other hand, updates the values above the pinch point and takes into account the amount of heat released ($Qcond$) by the condensers.

$\forall\, y \in [1, ZonePinch - 1], \forall\, j \in [1, S_y]$

$$NHL_{y,j} = Q_{y,j} - \sum_{\substack{i \in [j,\, S_y] \\ j \in S_y}} \left(Qevap_{y,i}\right) - \sum_{\substack{y \neq ZonePinch-1 \\ z \in [y+1,\ ZonePinch-1] \\ k \in [1, S_z]}} (Qevap_{z,k}) \qquad (2)$$

$\forall\, y \in [ZonePinch, Z],\ \forall\, j \in \left[1, S_y\right]$

$$NHL_{y,j} = Q_{y,j} - \sum_{\substack{i \in [1\,,\,j] \\ j \in S_y}} (Qcond_{y,i}) - \sum_{\substack{y \neq ZonePinch \\ z \in [ZonePinch,\ y-1] \\ k \in [1, S_Z]}} (Qcond_{z,k}) \qquad (3)$$

After positioning all HP, the electricity consumption ($Welec$) by these units must now be determined. Eq. (4) is derived by rearranging the coefficient of performance (COP) formula. Note that the amount of electrical energy consumed by the compressor is represented by the (y, j) coordinates of the evaporator. This is why the equation for electricity consumption is analyzed only below the pinch point.

$\forall\, y \in [1,\ ZonePinch\ - 1],\ \forall\, j \in \left[1, S_y\right]$

$$Welec_{y,j} = \sum_{\substack{z \in [ZonePinch,\ Z] \\ k \in [1, S_Z]}} \left(\frac{Qevap_{y,j}}{COP_{y,j,z,k} - 1} \right) \qquad (4)$$

To ensure coherent design and operation, several limiting parameters must be controlled in HP systems [10]. This model focuses on controlling two parameters: condenser temperature (T_{cond}) and temperature lift difference (ΔT_{lift}), which is the difference between the condenser and evaporator temperatures. Different refrigerants and compressor architectures impose operating limits on these parameters.

$$T_{z,k} - T_{y,j} < \Delta T_{lift\,max} \qquad (5)$$

$$T_{z,k} < T_{cond\,max} \qquad (6)$$

Eq. (5) and Eq. (6) show the constraints included in the model to guarantee that the HP adhere to the parameters set by the user.

The primary objective of HP utilization is process electrification, aiming at the minimization of thermal energy consumption. To establish a correlation between electrical and thermal power, the objective function criterion is defined based on process exergy using a conversion factor corresponding to the inverse of Carnot efficiency. The adoption of this factor preserves the physical consistency of the objective function and ensures it yields the expected results. This is the main distinction from the objective function proposed in the reference article [8], which did not adequately favor process electrification. This limitation was demonstrated by comparing two hypothetical cases with inverted heat and electricity utility values, for which the original formulation did not yield the expected results. The objective function adopted in the present work is presented in Eq. (7).

$$z = NHL_{1,1} * \begin{Bmatrix} 0, & If\ T_{1,1} > T_0 \\ \frac{T_{1,1}}{T_0 - T_{1,1}}, & If\ T_{1,1} < T_0 \end{Bmatrix} + NHL_{Z,S_Z} * \frac{T_{Z,S_Z}}{T_{Z,S_Z} - T_0} + \sum_{y \in [1,\ Z]} \sum_{j \in [1,\ S_Z]} Welec_{y,j} \qquad (7)$$

The intention is to minimize z. The first term of the equation represents the exergy impact associated with the use of a cold utility ($NHL_{1,1}$). This term is only considered when the initial temperature of the GCC ($T_{1,1}$) is lower than the ambient temperature (T_0), which indicates the use of a specific, costly cold utility. Otherwise, simple cooling water is used, rendering this impact negligible. The second term corresponds to the impact exerted by the hot utility (NHL_{Z,S_Z}). Therefore, the exergy term is calculated using the ambient temperature (T_0).

Finally, the third term of the equation accounts for the impact of electrical energy consumption ($Welec$). The equation as a whole thus enables the conversion of enthalpy balances into exergy balances: the enthalpy flows are modulated by a Carnot factor, which reflects the degradation of energy quality with temperature — whether the system operates as a heat engine in hot or cold mode — while electrical energy, being pure exergy, is directly integrated without any additional correction.

The results obtained from the OPTI-PAC module for the GCC must be converted by treating the heat pump as a utility stream (cold for the evaporator and hot for the condenser). The temperature values obtained from the GCC correspond to the intermediate temperature (T^*) of the process streams. To express this value in terms of the refrigerant fluid temperature, a term of $\Delta T_{min}/2$ must be added for a cold stream and subtracted for a hot stream [5]. These values are therefore converted into their respective hot and cold stream temperatures, as expressed in Eq. (8) and Eq. (9).

$$T_{evap,RF} = T^*_{evap} - \frac{\Delta T_{min}}{2} \qquad (8)$$

$$T_{cond,RFP} = T^*_{cond} + \frac{\Delta T_{min}}{2} \qquad (9)$$

2.2. Heat pump topological placement & heat exchanger network design

In the second step the HEN can then be modelled, allowing the connections between the streams introduced by the heat pump and the existing process streams to be visualized and analyzed. The Opti-PAC model then

generates results which are exported to the Opti-REc model. Opti-REc Model implement a MILP model dedicated to the optimal synthesis of Heat Exchanger Network [11]. This model requires the list of hot and cold stream to be integrated that is completed by the Heat Pump condenser and evaporator. Since latent heat transfer is involved, a temperature difference of 0.01 K is imposed to simulate the stream as pseudo-sensible heat transfer, as required by the model formulation. In the model, constraints are introduced that prohibit the condenser and evaporator streams of the heat pump from being connected to hot or cold utilities. As a result, these streams may only be connected to process streams.

Taking these considerations into account, the resulting heat exchanger network (HEN) is composed of a set of heat exchangers connecting the condensers and evaporators of each heat pump to the process cold and hot streams, respectively, and also includes integration heat exchangers between process hot and cold streams.

To be implemented in practice, a HEN must represent an appropriate compromise between energy recovery and capital cost. For this reason, the Opti-REc model allows the HEN to be *relaxed*, meaning that the number of integration heat exchangers can be reduced by accepting a higher energy consumption. It is therefore important to note that the resulting HEN does not necessarily achieve the Minimum Energy Requirement (MinER). Conversely, to identify a balanced trade-off between heat recovery and CAPEX, the methodology proposed by [11] is applied. This approach evaluates the impact of the number of integration heat exchangers (IHEs) on the recovered energy.

2.3. Simulation

In order to integrate the heat pump into the simulation, it is first necessary to select a refrigerant fluid, the choice of which is not determined by the preceding approaches, and then to determine its thermodynamic properties, after which the heat pump can be incorporated into the simulation model.

2.3.1. Selecting the refrigerant fluid

The selection of the refrigerant fluid relies on the evaporator and condenser temperatures that are directly derived from the results of the first MILP model that can be calculated through Eq. (8) and Eq. (9), respectively. Based on these results, thermodynamic properties are investigated in order to identify a fluid that is compatible with the operating conditions of the case under study. In particular, fluid that can evaporate and condense at the required temperature while consistent parameters for heat pump applications have been considered [10]. Once the refrigerant fluid has been selected, thermodynamic calculations are performed to determine the required refrigerant mass flow rate to satisfy the heat pump's energy demands across its three main components: the compressor, the evaporator and the condenser. As these values may differ for each component, the highest is adopted to ensure that all thermal and mechanical requirements are met throughout the simulation.

2.3.2. Simulation with heat pump integration

In the previous steps, the models assume that the heat capacity flow rates (FCp) of the streams remain constant over the considered temperature interval. To relax this assumption and adjust the heat duties and temperatures of the Heat Exchanger Network, a final step is performed. Once the refrigerant has been selected, the corresponding mass and heat balances as well as the thermodynamic properties are computed using the ProSim Plus software [12]. The characteristic parameters of the heat pump components namely the evaporator, compressor, condenser, and expansion valve are then incorporated into the model. When required, separators and mixers are also introduced to represent configurations in which the heat pump evaporator or condenser is connected to more than one process stream.

3. Case study

The selected case study concerns the oil pretreatment step of a biodiesel refining process [13]. Figure 4 displays the process flow diagram of the process. The crude oil is initially heated before being mixed with the other reagents: sodium hydroxide, phosphoric acid, and water. Then, the mixture is centrifuged to remove gums (phospholipids). The product of this separation step is heated before entering a second separation stage in which soap is removed by neutralizing free fatty acids. The remaining streams are reheated and depressurized for two vacuum drying stages. The products obtained from the drying stages must be cooled before storage. This brings the oil to the appropriate humidity level to initiate the esterification process. As observed in Figure 4, the process diagram can be divided into two main sections. The first corresponds to the pretreatment stage, dedicated to removing impurities, while the second corresponds to the oil drying section featuring two vacuum drying steps arranged in series.

The product that received pretreatment is rapeseed oil, which is primarily composed of triolein. Phosphoric acid and sodium hydroxide were modeled as water streams to facilitate the separation of impurities during the centrifugation stage and adjust the acidity of the product stream. These streams have very low flow rates, typically less than 1% of the total flow rate, so they do not significantly impact the material balance of the process. Consequently, the streams representing the removed impurities are specified by the plant as triolein and water mixtures, so it is not necessary to precisely define the reactions involved in these steps.

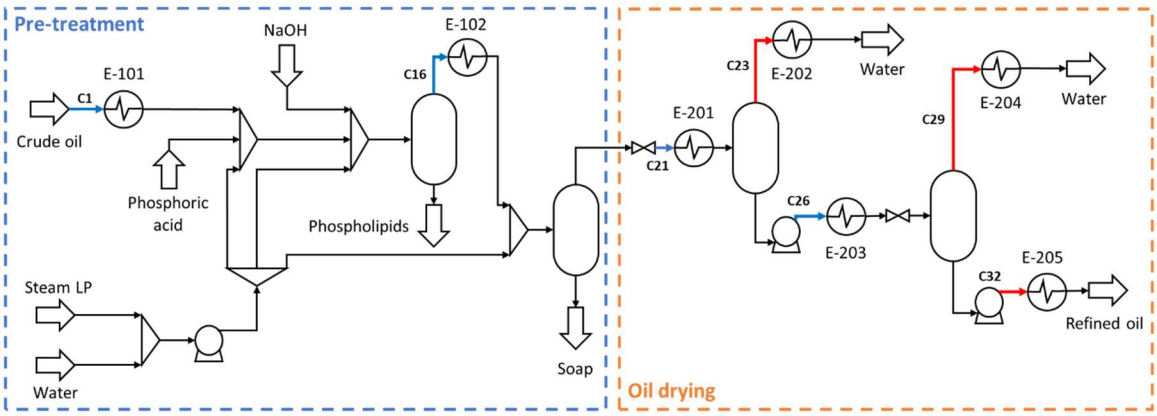

Figure. 4. *Process flow diagram for biodiesel refining pretreatment.*

This first configuration corresponds to the non-integrated process: process streams C1, C16, C21 and C26 are cold streams of the process and are connected to hot utilities. Meanwhile, C23, C29 and C32 are used to cool the hot streams process and are connected to cold utilities. Table 1 summarizes the streams data for the process.

Table 1. *Hot and cold stream data.*

Process stream	Type process stream	Required heat	Heat transfer, kW	F*Cp, kW/K	Tin, K	Tout, K
C1	Cold	Sensible heat	315.81	5.74	303.15	358.15
C16	Cold	Sensible heat	76.32	6.41	356.24	368.15
C21	Cold	Latent heat	360.37	36037.10	349.02	349.03
C23	Hot	Latent heat	491.92	49192.49	349.03	349.02
C26	Cold	Sensible heat	37.25	5.72	349.64	356.15
C29a	Hot	Sensible heat	1.26	0.025	352.33	302.11
C29b	Hot	Latent heat	32.49	3248.99	302.11	302.10
C32	Hot	Sensible heat	69.18	5.38	353.00	340.15

3.1. Heat pump placement

3.1.1. Pinch Analysis and GCC

A pinch analysis was conducted based on the data presented in Table 1 and assuming a minimum temperature difference (ΔTmin) of 20 °C for all heat exchangers. The resulting GCC, shown in Figure 5, reveals two PPP: a main pinch point positioned at 339.03 K and a secondary one located below it where an energy pocket is observed at 313.15 K. The system also has a minimum energy requirement (MinER) of 619.67 kW for the hot utility (U_H) and 424.77 kW for the cold utility (U_c).

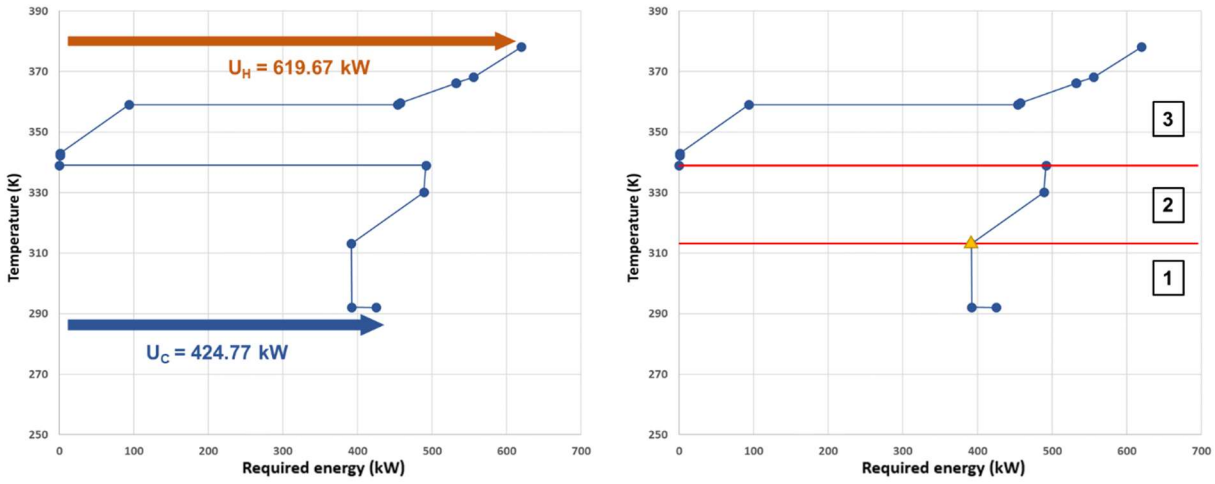

(a) *(b)*

Figure. 5. *GCC in the case study: a) Emphasis on required energy for the MER, b) GCC zone division.*

Ambient temperatures are higher than $T_{1,1}$, the cold utility temperature (292.11 K). Therefore, the cost of the cold utility does not need to be considered in the objective function. Under this condition, the water supply can be used directly as the cold utility because its cost is negligible compared to the hot utility's cost. Consequently, it does not significantly impact the analysis of thermal integration.

3.1.2. Heat pumps placement: MILP results

The first step of the methodology consists in determining the optimal number and (Q, T) placement of heat(s) pump(s). For that purpose, the GCC is discretized with a temperature interval of 1 K to allow for greater flexibility on the placement of heat pumps. This leads to 33 segments in Zone 1, spanning from the start of the data to the potential pinch point, 49 segments in Zone 2, between the potential pinch point and the pinch point, and 67 segments in Zone 3, above the pinch point. Moreover, design specifications include a $T_{cond\ max}$ of 400 K and a $\Delta T_{lift\ max}$ of 21 K.

Notably, these HP design conditions are consistent with industrial standards for this technology [10]. Also, a sensitivity analysis was performed to determine the best ΔT lift value, in which the parameter was systematically varied over the range of 20 to 30 K. This analysis identified 21 K as the optimal value, as it maximises recovery efficiency while requiring the lowest ΔT lift. Once these inputs have been defined, the optimization procedure can be launched to determine the optimal placement of the HP within the GCC. Figure 6 illustrates the resulting configurations for one (Figure 6a) and two HPs (Figure 6b), respectively.

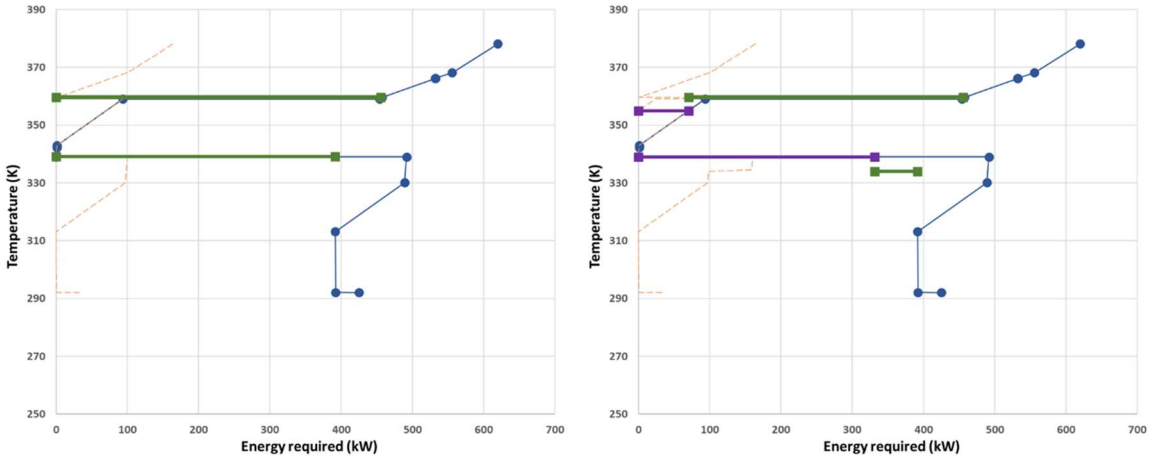

(a) *(b)*

Figure. 6. *Optimal solution for the example: a) 1 HP, b) 2 HP.*

In the figures, the green and purple markers correspond to HP1 and HP2 respectively. The segment located below the pinch point represents the evaporator, while the segment above it corresponds to the condenser of each heat pump. The GCC modified by the integration of the heat pumps is depicted by the orange dash line. The thermodynamic characteristics of the HP identified in the figures are summarized in Tables 2 and 3.

Table 2. *Thermodynamic characteristics in the optimal solution for 1 HP*

HP ID	$T_{evap,P}$,K	$T_{cond,P}$, K	Qevap, kW	Qcond, kW	Welec, kW	COP
1	339.02	359.64	391.76	455.51	63.75	7.15

Table 3. *Thermodynamic characteristics in the optimal solution for 2 HP*

HP ID	$T_{evap,P}$,K	$T_{cond,P}$, K	Qevap, kW	Qcond, kW	Welec, kW	COP
1	334.03	355.01	60.22	70.31	10.08	6.97
2	339.02	359.64	331.54	385.49	53.95	7.15

As shown in Figure 6a, the single HP configuration already substantially reduces the hot utility requirement, decreasing it from 619.67 kW to 164.16 kW, with an electrical consumption of 63.75 kW. As highlighted in Figure 6b, although the addition of a second heat pump further slightly reduces the hot utility demand, its integration is less economically viable due to the associated capital compared to the first unit reduction, due to the increased number of heat exchangers and heat pumps integrated into the network. Consequently, the configuration with a single heat pump, illustrated in Figure 6a, represents the most practical option.

The addition of a heat pump to a HEN is an important strategy for reducing the Minimum Energy Requirement (MER), and the improvement achieved for the present case study is illustrated in Figure 7.

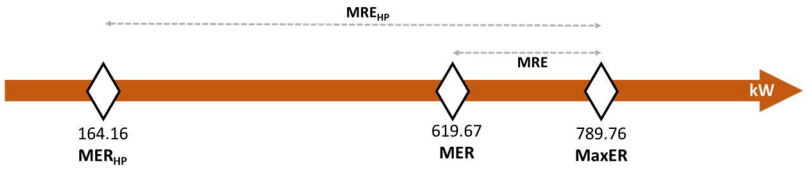

Figure. 7. *Target Impact of the Heat Pump on the Maximum Recoverable Energy.*

The benefits of heat pump integration become even more evident in Figure 7, where the presented case study considerably benefits from its application, yielding an energy integration potential 3.5 times greater when comparing the two MRE values.

3.2 Heat pump topologic placement & heat exchanger network design

Integrating a HP into a HEN is complex due to the connection of the condenser and evaporator to the process streams. To incorporate the heat exchangers corresponding to the heat pump, two additional streams are added to the original list: one associated with the evaporating refrigerant fluid and one with the same condensing refrigerant fluid. The corresponding temperature values are corrected by means of Eq. (8) and Eq. (9), while the heat capacity flow rate (F*Cp) is derived from the heat duty obtained as an output of the model. Table 4 presents the heat pump streams considered in the analysis.

Table 4. *New hot and cold stream data with heat pumps.*

Process stream	Type of stream	Type of heat exchanged	Heat transfer, kW	F*Cp, kW/K	Tin, K	Tout, K	N_{int}	N_{div}
Evaporator	Cold	Latent heat	391.76	39175.72	329.02	329.03	1	2
Condenser	Hot	Latent heat	455.51	45550.86	369.64	369.63	1	2

Furthermore, the last two columns report the variables that must be defined by the user within the Opti-REc module: N_{int}, which defines the maximum number of temperature interval allowed for a given stream, and N_{div}, which sets the maximum number of divisions allowed for each temperature interval. Figure 8 presents this explanation in a more visual manner. It is worth noting that the heat pump streams cannot have N_{int} values other than 1, while variations in N_{div} values are permitted. For the present case study, the system yields no feasible solution when N_{div} is equal to 1, which is why a value of 2 is adopted. The absence of a feasible solution for N_{div} = 1 will be further justified later in this work.

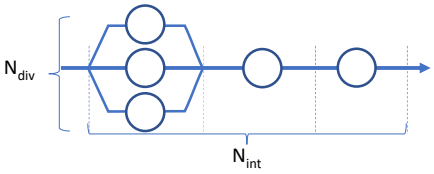

Figure. 8. *Stream parameters in Opti-REc module.*

To determine the most favourable configuration for process implementation, a study consisting in increasing the number of IHEs was conducted in order to assess the impact of this parameter to the relative recovered energy (rRE). The rRE is a Key Performance Indicator defined by Eq. (10) and illustrated by Figure 10, which presents the variation of this parameter as a function of the number of integration heat exchangers.

$$rRE = \frac{SolutionRE_{HP}}{MRE_{HP}} = \frac{MaxER - UH_{HP}}{MaxER - MER_{HP}} \qquad (10)$$

To complement this parameter, Figure 9 shows the hot utility requirement for each configuration with 2, 3, and 4 integrated heat exchangers (IHE). It is worth noting that the subsequent values are very close to the MER value (164.16 kW), as presented in Figure 10.

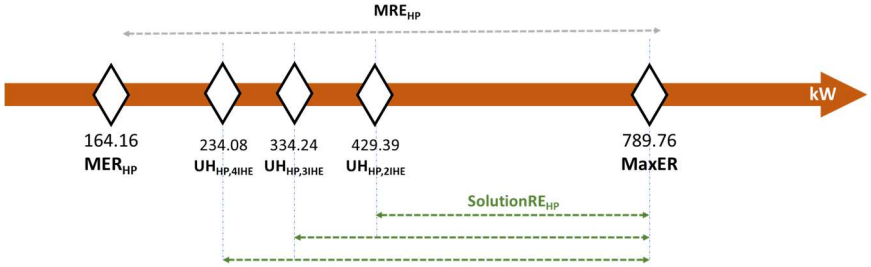

Figure. 9. *Variation of Recovery Energy with 1, 2 and 3 IHE.*

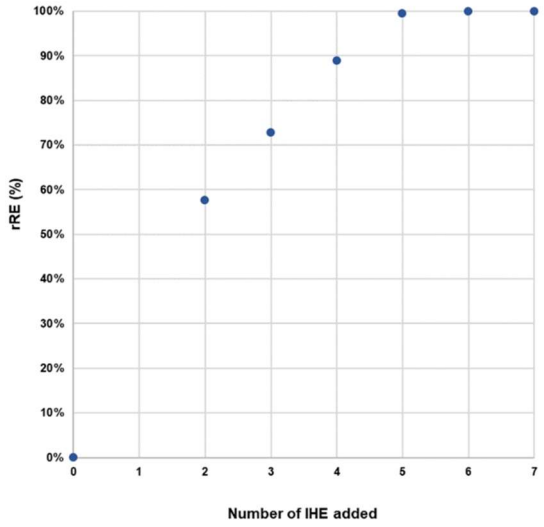

Figure. 10. *Variation in rRE as a function of the number of integration heat exchangers to the process.*

The graph shows that the configuration including only the HP already leads to a very significant energy recovery (rRE > 50 %). The incorporation of a heat pump comprising three heat exchangers into the system results in a progressive energy gain with the addition of the 4th and 5th heat exchangers, followed by a marginal gain for the remaining two units. Therefore, to find the right balance between capital expenditure (CAPEX) and energy efficiency, configurations exceeding 80% of the MaxER are optimal [11].

The best configuration obtained with the heat pump includes one integration heat exchanger in addition to the three heat exchangers inherent to the heat pump itself. This is possible imposing a maximum of 4 integration heat exchangers (two for the condenser, one for the evaporator and one linked with the process in both sides) which leads to the arrangement shown in Figure 11.

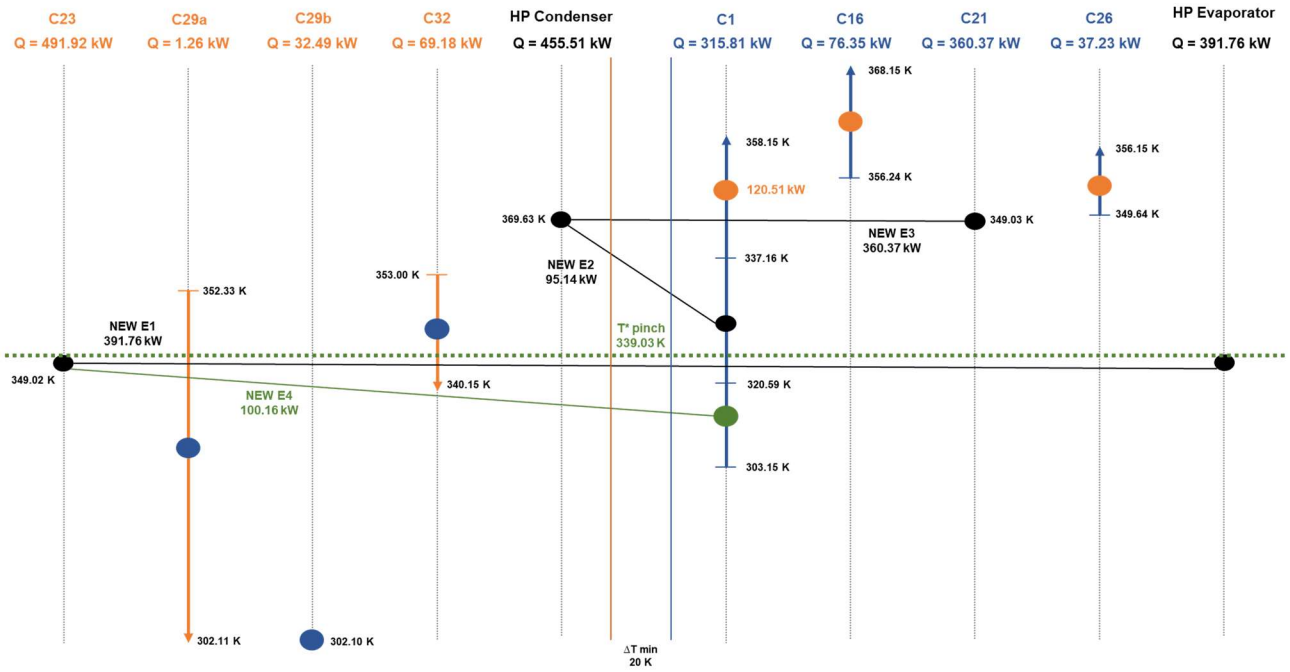

Figure. 11. *Relaxed HEN with HP via the Opti-REc software.*

In Figure 11, hot streams are shown as orange arrows and the cold streams as blue arrows. The integration Heat exchanger (IHE) is represented by a green circle, while cold utilities appear as blue circles connected to hot streams, and hot utilities as orange circles connected to cold streams. With the selected configuration, the process requires 234.08 kW of hot utility in exchange for 63.75 kW of electrical energy.

3.3 Simulation

Based on the results obtained, the system was coupled with the HP through simulation in ProSimPlus software [12].

3.3.1. Choosing the refrigerant fluid

Using the temperature conversion relation given in Equations 10 and 11, the evaporating temperature on the refrigerant fluid side ($T_{evap,\ RF}$) is 329.02 K, and the condenser temperature on the refrigerant fluid side ($T_{cond,\ RF}$) is 369.64 K. To meet the heat pump's thermal requirements, the refrigerant fluid must therefore evaporate at 329.02 K and condense at 369.64 K, operating between two distinct pressure levels. Under these conditions, the evaporator recovers 391.76 kW in the evaporator and the condenser delivers 455.51 kW with an electrical consumption of 63.75 kW. Based on the temperatures, the selected refrigerant fluid is 1,1,1,3,3-pentafluoropropane (R-245fa). The complete thermodynamic cycle is illustrated in Figure 12.

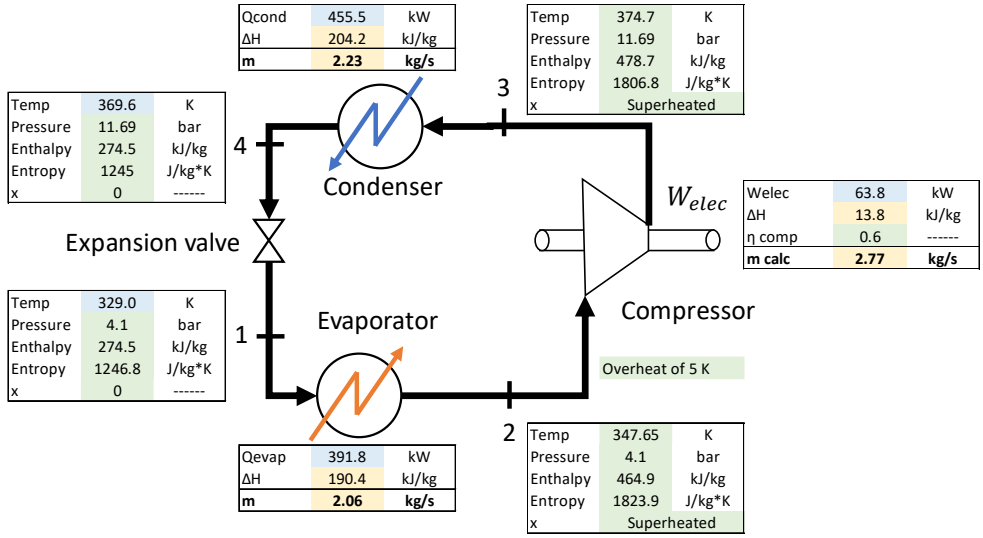

Figure. 12. *Thermodynamic cycle of R245fa refrigerant for the HP.*

The final process diagram is presented in Figure 13. To simplify visualization of the global process, the condenser and evaporator are presented separately, with the two individual heat exchangers explicitly depicted. It can be observed that the required refrigerant mass flowrate is 2.77 kg/s, and the heat pump operates between pressure levels of 4.1 bar and 11.69 bar. Following the selection of the refrigerant fluid, the heat pump was incorporated into the ProSim simulation model.

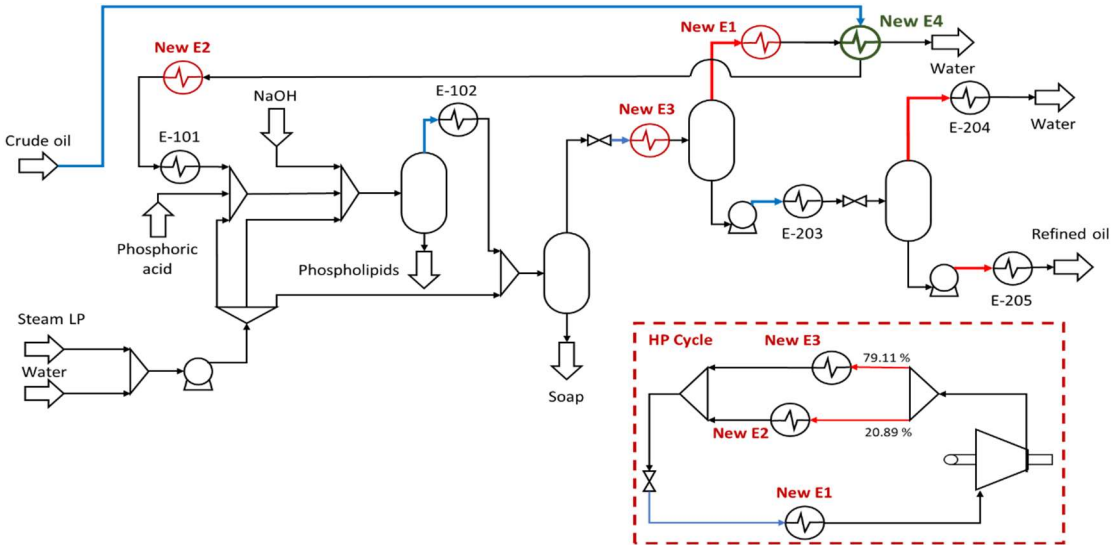

Figure. 13. *Process diagram incorporating the HP selected for the case study.*

In the diagram, the four new heat exchangers associated with the heat pump can be identified, along with the respective stream splits performed at the condenser and evaporator sides. The thermal duty distribution among these heat exchangers was determined based on the heat load assigned to each unit. Furthermore, it is worth noting that heat exchanger New E4 effectively replaces heat exchanger E-201, and heat exchanger New E1 replaces heat exchanger E-202. Moreover, heat exchanger New E3 reduces the utility demand of E-101, while New E2 decreases the thermal load of E-205. Although the resulting HEN is more complex, only two truly new heat exchangers are effectively added to the network

4. Conclusion

This study presented a systematic methodology for optimizing energy integration through heat pump placement in a biodiesel pretreatment process, combining pinch analysis, HEN synthesis, and simulation. The Opti-PAC model determined that a single heat pump represents the most practical configuration, reducing the hot utility demand from 619.67 kW to 164.16 kW with an electrical consumption of 63.75 kW and a COP of 7.15. The refrigerant R-245fa was selected for our example, and the final integrated process incorporates four heat exchangers into the process, with only two genuinely new units added. The results demonstrate that the proposed framework provides an effective and industrially coherent approach for minimizing external utility requirements, achieving an energy integration potential 3.5 times greater than the baseline configuration. Future work may extend the methodology to other utility technologies, such as combined heat and power systems or Organic Rankine Cycles, as well as more complex heat pump arrangements.

Nomenclature

$Welec$	electrical power, kW
$Qevap$	heat quantity evaporator, kW
$Qcond$	heat quantity condenser, kW
COP	coefficient of performance
$\Delta Tmin$	minimum temperature difference, K
NHL	new heat load values, kW
$\Delta Tlift$	temperature lift difference, K
F	mass flow rate, kg/s
Cp	specific heat capacity, kJ/(kg.K)
U_C	cold utility consumption, kW
U_H	heat quantity hot utility consumption, kW
IHE	integration heat exchanger
MaxER	Maximum Energy Requirement, kW
MER	Minimum Energy Requirement, kW
MRE	Maximum of Recoverable Energy, kW
U_H	Hot Utility Consumption, k

Subscripts and superscripts

RF	relative to refrigerant fluid
P	relative to process stream
y, z	relative to zones
j, k	relative to segments
HP	relative to HEN including heat pump
x_{IHE}	including x integration Heat exchanger

References

[1] International Energy Agency. Industry - Energy System [Internet]. International Energy Agency; 2025 [cited 2026 Mar 28]. Available from: https://www.iea.org/reports/energy-efficiency-2025#overview.

[2] COP30 Presidency Releases Executive Report and Outlines Next Steps to Accelerate Global Climate Implementation [Internet]. COP30 Presidency; 2026 [cited 2026 Mar 28]. p. 66. Available from: https://cop30.br/en/cop30-executive-report.

[3] Benstead R, Sharman FW. Heat pumps and pinch technology. Heat Recovery Systems and CHP. 1990;10(4):387–398.

[4] Linnhoff B, Hindmarsh E. The pinch design method for heat exchanger networks. Chemical Engineering Science. 1983;38(5):745–763.

[5] Robin Smith. Heat Exchanger Networks II: Energy Targets. Chemical Process Design and Integration. 2nd edition. 2016. p. 357–383.

[6] Thibault F, Zoughaib A, Jumel S. An Exergy-based MILP algorithm for Heat Pumps Integration in industrial processes. International Journal of Thermodynamics. 2014;17(3):156–161.

[7] Payet L. Remodelage de réseaux d'échangeurs de chaleur : collecte de données avancée, diagnostic énergétique et flexibilité [These]. Toulouse, INPT; 2018. Available from: https://theses.fr/2018INPT0149.

[8] Thibault F, Zoughaib A, Pelloux-Prayer S. A MILP algorithm for utilities pre-design based on the Pinch Analysis and an exergy criterion. Computers & Chemical Engineering. 2015;75:65–73.

[9] Linnhoff March. Introduction to Pinch Technology. Linnhoff March [Internet]. 1998 [cited 2026 Mar 30];

[10] Jouhara H, Żabnieńska-Góra A, Delpech B, et al. High-temperature heat pumps: Fundamentals, modelling approaches and applications. Energy. 2024;303:131882.

[11] Eneau C. Approche Générique couplant exergie, analyse pincement et optimisation pour l'évaluation des technologies émergentes - application aux procédés de conversions de CO2 en e-methanol [Internet] [thesis]. Université de Toulouse (2025). Available from: https://theses.fr/s416880.

[12] Fives ProSim S.A.S. ProSimPlus [Internet]. Labège, France; 2025 [cited 2026 Apr 19]. Available from: https://www.prosim.net.

[13] Gourmelon S. Méthodologie d'analyse et de rétro-conception pour l'amélioration énergétique des procédés industriels [Internet] [Theses]. Institut National Polytechnique de Toulouse - INPT; 2015 [cited 2025 Dec 5]. Available from: https://theses.hal.science/tel-04237574.